THE JOURNAL OF PHYSICAL CHEMISTRY B

Article

pubs.acs.org/JPCB

NMR and Raman Spectroscopy Monitoring of Proton/Deuteron Exchange in Aqueous Solutions of Ionic Liquids Forming Hydrogen Bond: A Role of Anions, Self-Aggregation, and Mesophase Formation

Vytautas Klimavicius,[†] Zofia Gdaniec,[‡] Jonas Kausteklis,[†] Valdemaras Aleksa,[†] Kestutis Aidas,[†] and Vytautas Balevicius*[,†]

[†]Department of General Physics and Spectroscopy, Vilnius University, Sauletekio 9-3, LT-10222 Vilnius, Lithuania

[‡]Institute of Bioorganic Chemistry, Polish Academy of Sciences, Z. Noskowskiego 12/14, PL-61704 Poznan, Poland

ABSTRACT: The H/D exchange process in the imidazolium-based room temperature ionic liquids (RTILs) 1-decyl-3-methyl-imidazolium bromide- and chloride ([C_{10}mim][Br] and [C_{10}mim][Cl]) in D_2O solutions of various concentrations was studied applying ^1H, ^{13}C NMR, and Raman spectroscopy. The time dependencies of integral intensities in NMR spectra indicate that the H/D exchange in [C_{10}mim][Br] at very high dilution (10^{-4} mole fraction of RTIL) runs only slightly faster than in [C_{10}mim][Cl]. The kinetics of this process drastically changes above critical aggregation concentration (CAC). The time required to reach the apparent reaction saturation regime in the solutions of 0.01 mole fraction of RTIL was less 10 h for [C_{10}mim][Br], whereas no such features were seen for [C_{10}mim][Cl] even tens of days after the sample was prepared. The H/D exchange was not observed in the liquid crystalline gel mesophase. The role of anions, self-aggregation (micellization), and mesophase formation has been discussed. Crucial influence of Br^- and Cl^- anions on the H/D exchange rates above CAC could be related to the short-range ordering and molecular microdynamics, in particular that of water molecules. The concept of the conformational changes coupled with the H/D exchange in imidazolium-based ionic liquids with longer hydrocarbon chains can be rejected in the light of ^{13}C NMR experiment. The revealed changes in ^{13}C NMR spectra are caused by the secondary (^{13}C) isotope effects not being the signal shifts due to the conformational *trans*−*gauche* transition.

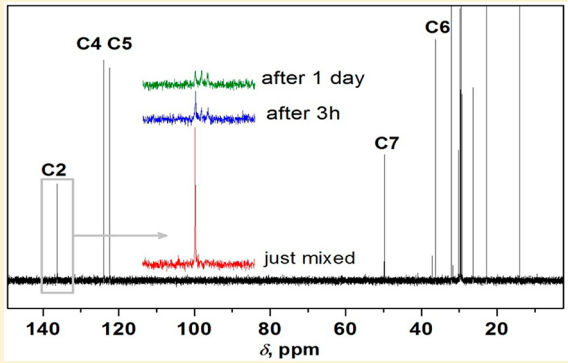

INTRODUCTION

Ionic liquids (ILs)/room temperature ionic liquids (RTILs) can be considered as one of the most successful breakthroughs creating smart materials and multifunctional compositions possessing many appealing features important for the applications in high technologies, including various artificial sensors of new generation, electrochemistry, fuel cells and batteries, (bio-) catalysis, *etc.*[1−4] Nevertheless, the processes taking place in ionic liquids are not completely understood on a molecular level and constitute one of the main challenges in fundamental research. Hydrogen bonding between the anions and cations in certain ILs can play crucial role. Localized and directionally depending H-bonding disorder the Coulomb network, and the system then deviates from the charge symmetry.[5] This intensifies the ionic dynamics and results in a significant decrease of melting points and viscosity. Hence, some important macroscopic properties of ILs can be tuned by adjusting the ratio between Coulomb- and the H-bond contributions, even the latter being energetically less significant.

Ionic liquids are intriguing systems to study in respect of purely H-bonding phenomena. In many of ILs the anions are the conjugate bases of various acids, in certain cases, strong and very strong, as for example, halogenides (Cl^-, Br^-), trifluoroacetate (CF_3COO^-), triflate ($CF_3SO_3^-$), *etc.*[6] Hence, some of ILs can be conceptualized as ionic pair systems $A^-\cdots H^+B$ created by very 'deep' proton transfer from the acid (A) to the defined base (B). These ionic pairs are kind of 'inverted' in respect of the traditional ones that appear in numerous H-bond systems with proton transfer.[7−10] Such ILs structures can be thought as the 'ground state' that can be disturbed by various external stimuli (temperature, media effects, *etc*) reversing the proton migration toward the anion and maybe even culminating with the return of the system to the neutral H-bond A−H···B. If this succeeded, the novel sort of phase transitions could be expected that would create the hybrid state of matter with the properties that occupy an intermediate place between ionic and nonionic liquids. The studies of proton/deuteron (H/D) exchange trying to determine the possible pathways of this reaction and its kinetics would provide extremely valuable information on the picture of H-bond in ILs, including the large amplitude proton motion and thus

Received: March 1, 2013
Revised: August 9, 2013
Published: August 12, 2013

evaluating the chances to provoke the reverse proton migration by proper physically realizable stimuli.

The cation−anion interactions and various aspects of H/D exchange reactions in some imidazolium-based ILs have been studied by means of X-ray photoelectron, NMR, and Raman spectroscopy techniques.[11−16] Several intriguing findings can be listed. For example, charge transfer is not related to H-bonding; however, both H-bonding and charge transfer are seen to be enhanced for small and more strongly coordinating anions;[11] the relation between the slowdown of rotational dynamics and the H/D exchange deactivation has been deduced;[12] complex dependency of the H/D exchange rates on RTIL concentration in water has been observed;[13] anomalous dynamics of ions at very low ionic liquid concentration in D_2O has been revealed;[14] the H/D exchange has induced conformational changes of ILs;[15] the rate of H/D exchange, diffusion coefficients, and spin−lattice relaxation time are affected by critical aggregation of RTILs.[16]

The purposes of present work were (i) to study the anion, self-aggregation, and mesophase effects on the H/D exchange in the 1-decyl-3-methyl-imidazolium bromide- and chloride ([C_{10}mim][Br] and [C_{10}mim][Cl], respectively) in D_2O solution below and above critical aggregation concentration as well as in the liquid crystalline gel mesophase by means of the ^1H, ^{13}C NMR, and Raman spectroscopy and (ii) to check the possibility of conformational changes induced by the H/D exchange in imidazolium-based RTILs with longer alkyl chains.

EXPERIMENTAL SECTION

The 1-decyl-3-methyl-imidazolium bromide and chloride from Merck KGaA Darmstadt and from Ionic Liquids Technologies GmbH (the structure and atom numbering are shown in Figure 1) were dried under vacuum at 80 °C for one day; D_2O (99%, Aldrich) was used without additional treatment. The samples were prepared by weighting (±0.1 mg) the components.

NMR experiments were carried out on Bruker Avance^{II}/400 and Bruker Avance^{III}/500 NMR spectrometers operating at 400/500 and 100/125 MHz for ^1H and ^{13}C, respectively, using 5 mm BBO probe-heads. The temperature of 298 K was controlled with an accuracy of ±0.5 K. The signals of D_2O solution and DMSO in capillary insert were used as the reference and then converted in δ-scale, with respect to TMS, taking their chemical shift values from ref 17. The D_2O and DMSO were also used for locking.

Raman spectra were obtained using Bruker MultiRAM FT-Raman spectrometer with motorized xyz-sample stage and with liquid nitrogen cooled germanium detector. The 1064 nm wavelength beam of the pulsed Nd:YAG laser (500 mW) was used as the excitation source. The 180° scattering geometry was employed. The resolution of the spectrometer was set to 2 cm^{-1}. The Raman spectra were recorded in the 70−4000 cm^{-1} spectral range at 296 K. Some samples were cooled down up to 49 K. FT-Raman spectrometer control and experimental data digital processing were performed using the OPUS 6.5 software program package.

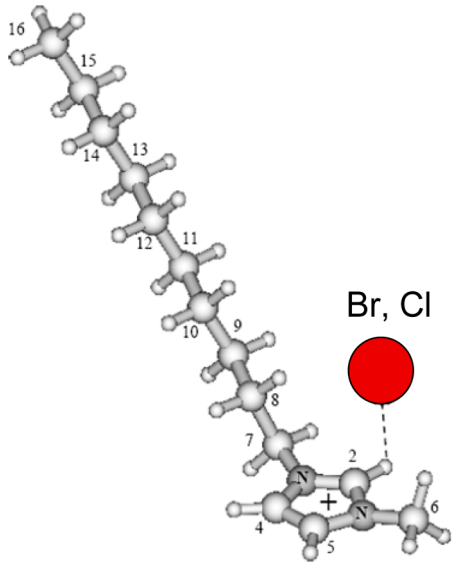

Figure 1. Molecular structure and carbon numbering of [C_{10}mim][X], X = Br, Cl.

COMPUTATIONAL DETAILS

Electronic structure calculations were conducted using Gaussian09 program.[18] Equilibrium geometries and harmonic vibrational frequencies as well as Raman activities of the 1-butyl-3-methyl-imidazolium cation isotopologues are based on the calculations using the B3LYP exchange-correlation functional[19] and the 6-311++G** basis set.[20] Bulk solvent effects are accounted for by using a polarizable continuum model (PCM).[21] Default settings of PCM were utilized apart from parameters *ofac* and *rmim*, which were assigned values of 0.8 and 0.5, respectively. Anharmonic analysis was performed at the B3LYP/6-31G* level *in vacuo* using second order perturbative approach[22] implemented in Gaussian09. ^1H and ^{13}C magnetic shielding tensors were calculated at the level of PBE0/6-311++G(2d,2p)/PCM. More details concerning this choice are given in ref 6.

RESULTS AND DISCUSSION

Phase Behavior and Sample Compositions. It is well-known that some of imidazolium-based RTILs [$C_n$mim][X] with sufficiently long alkyl chains (n = 6−18) demonstrate a broad variety of phenomena in the phase behavior[23−26] and the aggregation (micellization) processes.[27−33] More details are known regarding the studied compounds. The addition of water to [C_{10}mim][Br] causes its conversion from a viscous liquid to a gel possessing the optical birefringence.[23] The coexisting mesophases for closely related [C_{12}mim][Br] were identified more precisely being as solid, lamellar, and hexagonal ones.[24] At the higher content of water (~15% w/w of H_2O), both [C_{10}mim][Br]/H_2O and [C_{10}mim][Cl]/H_2O solutions convert into hardened gel, which resists flow upon gravity, already at room temperature. Some serious technical problems, such as difficulties to fill the NMR tubes with the hardened substance, the inserting of the lock-capillary, and others, have been met during experiments on gel samples as already reported by us in ref 25. The mesophases disappear at further dilution, and the viscosity of the solutions drops drastically. This highly diluted state (below ~0.05−0.08 mole fraction of RTIL) was called as the aqueous solution.[23] The coexisting solid and liquid phases can appear only below ~290 K.[26]

It is obvious that the rates of H/D exchange process in such RTILs can be crucially influenced by the phase behavior when different molecular sites and peculiar environments in the microscopic or mesoscopic scales appear. For example, the imidazolium groups can get blocked inside of inverted

dx.doi.org/10.1021/jp4021245 | J. Phys. Chem. B 2013, 117, 10211−10220

hexagonal structures, if such formed, or the formation of the regions with confined water (D_2O as deuteron donor) is enhanced due to the interplay between hydrophilic and hydrophobic segments, as well as the formation of the layered structures in the case of the lamellar phase.[24] In order to segregate the pure H-bond-driven contribution to the H/D exchange from possible phase/environmental effects, the composition of the samples should be chosen that makes sure that the systems are in the identical states. The aqueous solution phase (i.e., the one that is by many physical features very close to the 'classical' electrolyte (water + salt) system) would be most suitable. Therefore, two highly diluted samples of $[C_{10}mim][Br]$ and $[C_{10}mim][Cl]$ in D_2O (10^{-4} mole fraction of RTIL) have been first prepared and investigated.

Increasing the concentration in the aqueous solution phase the self-aggregation of some RTILs via micelle formation can take place,[27−33] even the mesophase formation is still excluded. This is important to study, as there are some indications that the rates of H/D exchange, diffusion coefficients, and spin−lattice relaxation time can sufficiently differ for the solutions being below and above of critical aggregation concentration (CAC).[16]

The C(2)−H···X^- bridge proton chemical shift dilution curves can provide useful information when determining the critical aggregation concentration, predicting structures of aggregates, *etc.*, as it was done for some $[C_nmim][X]$ series.[27−29] In those cases, the dilution curves exhibit a typical behavior with two linear dependencies of the chemical shift on concentration whose intersection reminds a break point. The corresponding concentration value is usually accepted as the CAC. In the case of $[C_{10}mim][Br]$ in H_2O, the break point of the chemical shift dilution curve was only roughly evaluated to be less than ∼0.01 mole fraction of RTIL.[25] In the present work, the CAC values have been determined more precisely for both studied compounds. The corresponding ^1H NMR shift break points are shown in Figure 2. This allowed us to determine the CAC values equal to 6.4×10^{-4} mole fraction and 9.9×10^{-4} mole fraction of $[C_{10}mim][Br]$ and $[C_{10}mim][Cl]$, respectively, which are in a perfect agreement with the available literature data (Table 1). Therefore, the next couple of samples of 0.01 mole fraction of RTIL in D_2O was prepared. Such composition assures that both systems are close to the midpoint between the onsets of aggregation and the gel mesopase formation. Also note that the samples of same composition were used studying the H/D exchange in some other RTIL systems (e.g. $[C_4mim][X]/D_2O$, X = I, BF_4).[34]

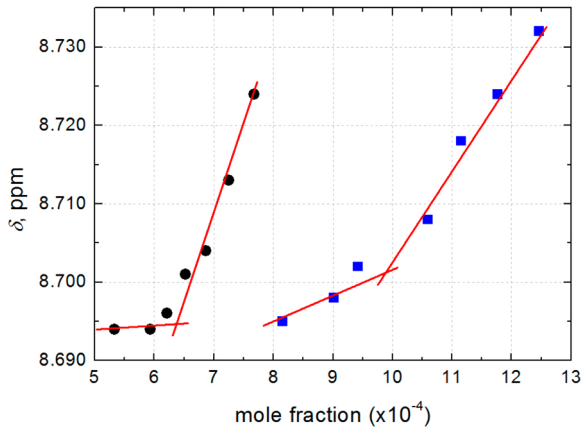

Figure 2. Determination of critical aggregation concentration (CAC) of $[C_{10}mim][X]$, X = Br (black circles), Cl (blue squares) using dependencies of chemical shift of C(2)−H···X^- proton on concentration in H_2O.

Table 1. Literature and Present Work Data on Critical Aggregation Concentration (CAC) of $[C_{10}mim][X]$, X = Br, Cl in H_2O and D_20 at 298 K

$[C_{10}mim][Br]$			$[C_{10}mim][Cl]$		
CAC, M	solvent and method	ref	CAC, M	solvent and method	ref
0.030−0.032	D_2O, NMR	29	0.055	H_2O, interfacial tension	27
0.029	H_2O, surface tension	32	0.045	H_2O, fluorescence	27
0.033	H_2O, conductivity	32	0.055	H_2O, NMR	27
0.04	H_2O, potentiometry	33	0.054	H_2O, surface tension	30
			0.060	H_2O, conductivity	30
CAC values recalculated to mole fraction: (5.3 − 7.2) × 10^{-4}			CAC values recalculated to mole fraction: (8 − 10) × 10^{-4}		
6.4×10^{-4} mole fraction	H_2O, NMR	present work	9.9×10^{-4} mole fraction	H_2O, NMR	present work

$[C_{10}mim][Br]/H_2O$ and $[C_{10}mim][Cl]/H_2O$ solutions convert at higher content of water from a viscous liquid to the anisotropic gel.[23,25] This gel was found to be stable over the range of ∼5−40% w/w of water (i.e., 0.08 - 0.53 mole fraction of RTIL). In order to check the influence of this mesophase on the H/D exchange rate another two samples of 0.4 mole fraction of RTIL in D_2O were prepared and investigated.

Monitoring of H/D Exchange Using ^1H and ^{13}C NMR. The experimental and calculated ^1H and ^{13}C NMR spectra of $[C_{10}mim][Br]$ in the neat RTIL as well as in various solvents and mesophases have been previously reported.[25,26,35] The ^1H and ^{13}C NMR spectra of $[C_{10}mim][Br]$ and $[C_{10}mim][Cl]$ (Figures 3 and 4) are very similar, and ^{13}C chemical shifts appear to be less sensitive to the anions used. Similar tendency has been observed for $[C_8mim][X]$ series with X = Br and Cl among those.[11] Instead of narrow symmetric peaks the broad more or less asymmetrically shaped signals are seen in ^1H NMR spectra registered in the gel phase (Figure 3). Such signal shapes are common for anisotropic liquids.[26] The greater ordering and more anisotropic character molecular motion in the gel phase is better pronounced in the spectrum of $[C_{10}mim][Cl]$ (Figure 3). The degree of asymmetry of the signal contours indicate that the biaxiality of this phase should be rather close to 1.[26]

The most remarkable changes during the H/D exchange have been observed for NMR signals of the imidazolium ring, as it could be *a priori* expected. This is particularly clearly manifested in ^{13}C NMR spectrum (Figure 4), where the signal corresponding to C(2) carbon atom splits into triplet characterized by $^1J(^{13}C-^2H)$ = 33.6 Hz due to $^{13}C-^2H$ spin coupling. The same value of $^1J(^{13}C-^2H)$ was obtained for both studied RTILs.

The kinetics of the H/D exchange was followed using the relative integral intensity of the ^1H NMR signal of C(2)−H proton normalized in respect to the peak of −C(16)H_3 group (Figure 5). This choice differs from that applied in ref 13, where the H/D exchange in $[C_4mim][BF_4]/D_2O$ mixtures was

dx.doi.org/10.1021/jp4021245 | J. Phys. Chem. B 2013, 117, 10211−10220

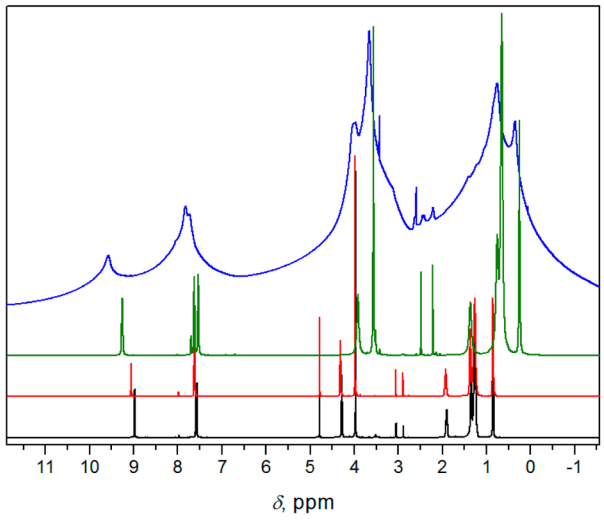

Figure 3. ^{1}H NMR spectra of [C_{10}mim][X] in D_2O solutions: close to the midpoint between the onset of aggregation and the gel formation (0.01 mole fraction of RTIL), X = Cl (black) and X = Br (red); in the gel phase (0.4 mole fraction of RTIL), X = Br (green) and X = Cl (blue); all at T = 298 K. The spectra below CAC are not shown because they inessential differ from those at 0.01 mole fraction of RTIL.

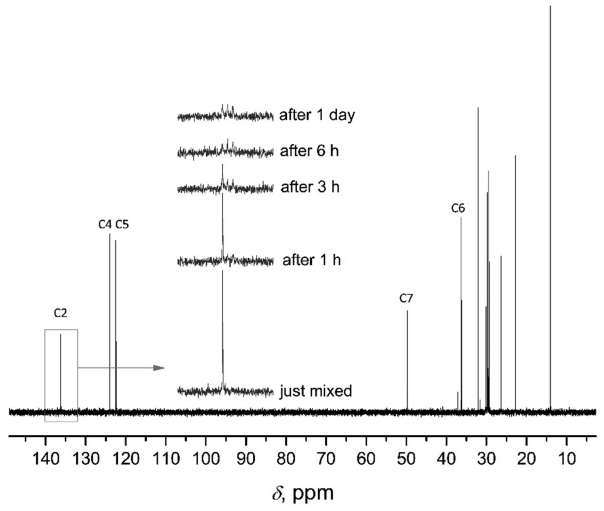

Figure 4. Monitoring of H/D exchange in ^{13}C NMR spectra of [C_{10}mim][Br] in D_2O solution (0.01 mole fraction of RTIL) at T = 298 K.

studied using the relative intensity of C(2)−H signal in respect to HDO. In our opinion, the signal of the terminal $-CH_3$ group is more appropriate because it provides more steady internal reference to normalize the integrals. The intensity of HDO peak can be affected by the H/D exchange between D_2O (i.e., solvent molecules) and traces of H_2O or other R−OH species that may be present in the mixtures as impurities, e.g. adsorbed from the air during the sample preparation when highly hygroscopic RTILs are used.

The H/D exchange rates are very different and depending on the sample composition (Figure 5). The time dependencies of integral intensities in ^{1}H NMR spectra indicate that the H/D exchange in [C_{10}mim][Br] at high dilution (10^{-4} mole fraction of RTIL) runs only slightly faster than in [C_{10}mim][Cl] (Figure 5, top graph). The kinetics of this process drastically changes

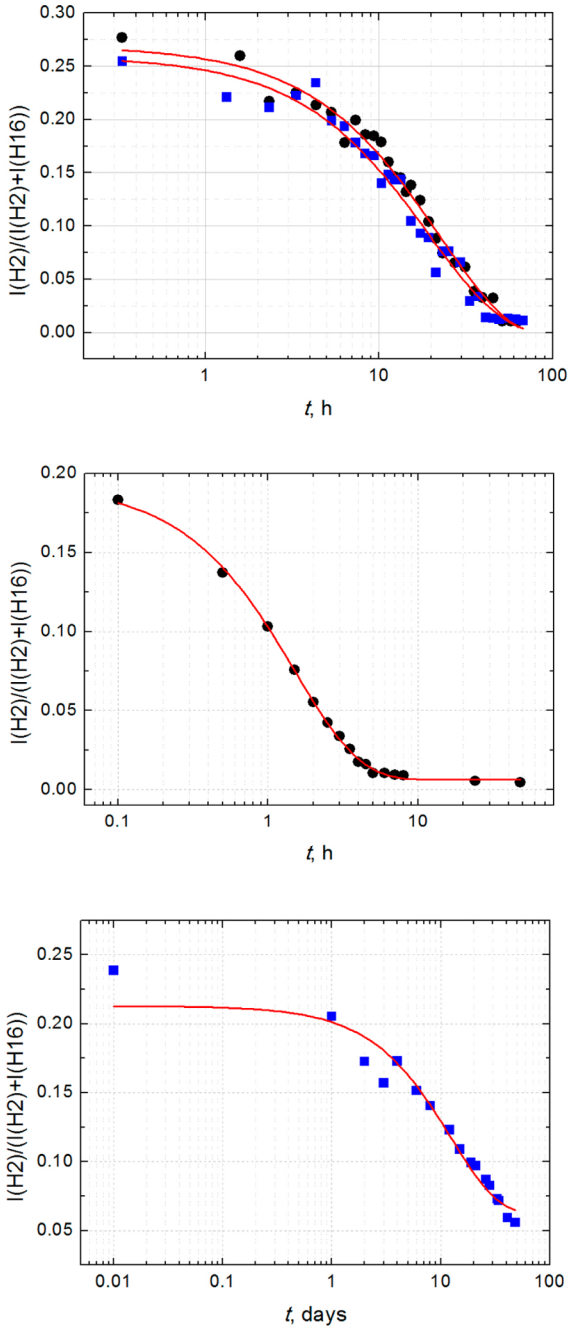

Figure 5. Kinetics of the H/D exchange reaction in [C_{10}mim][X], X = Br (black circles) and Cl (blue squares) in D_2O solutions at high dilution (10^{-4} mole fraction of RTIL, top graph) and above CAC (0.01 mole fraction, middle and bottom graphs) monitored using the relative integral intensity of ^{1}H NMR signal of C(2)−H proton respect to the signal of the terminal $-CH_3$ group.

above CAC. The time required to reach the apparent reaction saturation regime was less 10 h for [C_{10}mim][Br] (Figure 5, middle graph), whereas this reaction runs extremely slowly in [C_{10}mim][Cl]/D_2O solution (Figure 5, bottom graph). Such kinetics is comparable to that observed in [C_4mim][BF_4], where the time necessary to reach the apparent equilibrium state at certain D_2O concentrations was determined to be up to 40 days.[13,15] Note these our observations significantly differ from those in ref 16., where it was deduced that the fast H/D exchange does not occur in the solutions below CAC.

dx.doi.org/10.1021/jp4021245 | J. Phys. Chem. B 2013, 117, 10211−10220

It is interesting to compare the reaction rates in RTILs containing the same anions. According to the data reported in the literature for [C_4mim][Cl], the level of deuteration at C(2) site of 91% was achieved in a 1:20 weight ratio (~ 0.0056 mole fraction, i.e. close to the present work) in D_2O solution in 24 h, however, after rising the sample temperature.[36] A much faster kinetics observed in [C_{10}mim][Br]/D_2O solutions is comparable with the literature data for [C_4mim][I] reported in ref 33. The ^{1}H NMR signal corresponding to the C(2)−H proton disappears completely in 0.01 mole fraction solution in D_2O after 20 h.[34]

No changes in the intensity of ^{1}H NMR signal of C(2)−H proton were noticed for the gel samples (0.4 mole fraction of RTIL) during 48 days of observation from the sample preparation. Thus, we can state that this reaction does not run in the gel phase.

Comparison of other ^{1}H integrals to that of −C(16)H_3 resonance indicates that in imidazolium ring only C(2)−H proton is involved in the H/D exchange under the present experimental conditions. This is important to know because it is quite often assumed that anions can bind to all three imidazolium ring protons[35,36(and refs therein)] and thus they could also undergo the H/D exchange.

Secondary Isotope Effect on ^{13}C Chemical Shifts. The central line of the C(2)−D triplet is shifted in respect to the ^{13}C NMR signal of C(2)−H (Figure 4). This is due to the so-called secondary isotope effect, which has been studied in more detail. The secondary isotope effect, that is, the change of chemical shifts (δ) upon H/D substitution, originates from coupling of the proton and deuteron vibrational wave functions to the rest of the system.[37] In other words, the differences in the geometry of the A−H(D)···B bridge slightly affect the geometry and the local electron density in the rest of molecule and is reflected in the corresponding chemical shift values. The primary isotope effect $\delta_H - \delta_D$, depending on the nuclei involved and H-bond features, can be quite strong, for example, reaching up to ~0.5−0.7 ppm in the case of strong and short H-bonds, such as the intramolecular bonding in quinaldic- or picolinic acid N-oxides, intermolecular complexes of carboxylic acids with pyridine, *etc.*[37,38] The secondary isotope effects are usually much smaller than the primary ones, although in certain cases they can be comparable. For example, $|\delta_H - \delta_D|$ for some ^{13}C resonances in picolinic acid N-oxide reaches 0.47−0.57 ppm (depending on solvent) in comparison to the primary one of 0.48−0.78 ppm.[37] It is quite remarkable that this huge effect was observed for the carbon atom that is distant from the site of deuterium substitution by five chemical bonds, whereas for the carbons closer to the O−H(D)···O moiety the effect was much smaller (0.02−0.23 ppm).

In the present work, the secondary deuterium isotope effect on ^{13}C chemical shifts has been observed for H-bonded ionic liquid systems for the first time. However, the deuterium isotope effects on other nuclei have been already used for the study of H-bond in ionic liquids.[36] In a model system, selectively deuterated [C_4mim][Cl], this effect was found to be very significant for the $^{35/37}$Cl resonances (1.0−1.9 ppm) and practically negligible (0.002−0.004 ppm) for ^{1}H NMR signals. For [C_{10}mim][X], X = Br, Cl used in these studies, it is most pronounced for C(2) being 0.24−0.25 ppm (Table 2). This effect is within 0.02−0.05 ppm for other imidazolium ring and neighboring carbons and negligible for the rest of decyl chain from C(8) to C(16). Hence, the magnitude of the effect differs from that observed in the case of strong and short H-bonded systems.[37,38] Also note that the sign of the secondary (^{13}C) isotope effect is the same ($\delta_H - \delta_D > 0$) for all carbons.

Table 2. Chemical Shifts of Carbon Nuclei and Secondary (^{13}C) Isotope Effects $\delta_H - \delta_D$ (in ppm) in [C_{10}mim][X], X = Br, Cl in D_2O Solution at 298 K

	[C_{10}mim][Cl]			[C_{10}mim][Br]		
carbon no.	H[a]	D[a]	$\delta_H - \delta_D$	H	D	$\delta_H - \delta_D$
C(2)	136.23	135.98	0.25	136.28	136.04	0.24
C(4)	122.34	122.30	0.04	122.46	122.41	0.05
C(5)	124.03	123.98	0.04	124.01	123.97	0.04
C(6)	36.11	36.08	0.03	36.27	36.24	0.03
C(7)	49.72	49.69	0.03	49.78	49.76	0.02

[a]The label 'H' refers to the species with a proton in C(2)−H···X^- bonding, while 'D' refers to that with a deuteron.

These data are very useful when discussing the possibility of conformational changes revealed in other closely related RTILs by Raman spectroscopy[15,34,39,40] and also for the future theoretical treatment of H-bond dynamics in ionic liquids using 2D models with quantum averaging.[37]

Monitoring of H/D Exchange Using Raman Spectra. The sample composition of 0.01 mole fraction of RTIL in D_2O was high enough to carry out the registration of Raman spectra at the same conditions as it was set in NMR studies. The Raman studies are important in trying to reveal the possibility of anomalous conformational changes around the C(7)−C(8) bond (Figure 1) that seem to be coupled with H-bonding and H/D exchange processes.[15,39]

It is reasonable to suppose that the most comprehensive information concerning the H/D exchange should be obtained analyzing the band of C(2)−H stretching vibration (νC(2)−H). However, this band is strongly overlapped with other νC−H bands in the spectral range 2900−3100 cm^{-1}.[34,39] There is also a significant discrepancy between experimental and calculated vibrational frequencies at higher wavenumbers.[39,40] All these factors puzzle the reliable assignment of the modes, as for example, the polemic in refs 41 and 42, and make the processing of the band contours and the determination of their parameters more cumbersome. Therefore, the H/D exchange was monitored using the time evolution of the Raman bands at 1010 and 1024 cm^{-1} (Figure 6), assigned as the combination of the in-plane ring deformation and CH_3(N) deformation.[15,39] These bands have been successfully exploited for the same purpose in Raman studies of [C_4mim][[BF_4]/D_2O mixtures.[15] The time dependency of their integral intensities (Figure 7) indicates that the H/D exchange in [C_{10}mim][Br] is much faster than in [C_{10}mim][Cl]. The time required to reach the apparent reaction saturation regime was ~200 min for [C_{10}mim][Br], whereas no features reaching this were seen for [C_{10}mim][Cl] even at ~1000 min after the sample was prepared (Figure 7). Thus, the Raman spectroscopy results support the NMR ones (Figure 5).

Special attention has been paid in this work to the spectral range around ~600 cm^{-1} (Figure 8). The Raman bands at *ca.* 600 and 620 cm^{-1} are very often used studying the conformational changes in hydrocarbon chains attached to the imidazolium cation.[15,34,39,40] It was deduced that the conformation of the butyl chains depends on the type of anion,[34] the *trans*−*gauche* change can occur at the melting,[40] or it can be coupled with the H/D exchange.[15] The significant relative redistribution in the intensities at 602 and 625 cm^{-1} is clearly seen in the Raman spectra of both studied RTIL/D_2O

dx.doi.org/10.1021/jp4021245 | J. Phys. Chem. B 2013, 117, 10211−10220

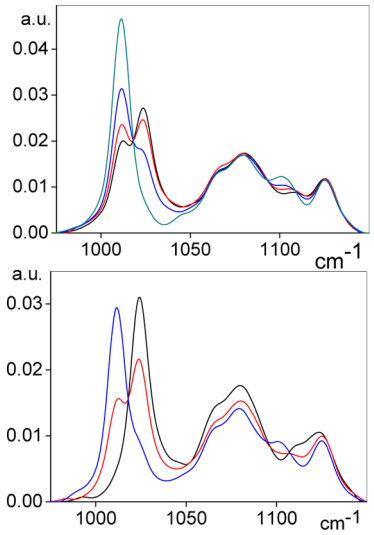

Figure 6. Monitoring of H/D exchange on the Raman bands at 1010 and 1024 cm^{-1} of $[C_{10}mim][X]$, X = Br (top; at 10 (black), 20 (red), 50 (blue), and 900 (green) min after the sample prepared) and Cl (bottom; at 10 (black), 200 (red), and 900 (blue) min) in D_2O solution (0.01 mole fraction of RTIL) at T = 296 K.

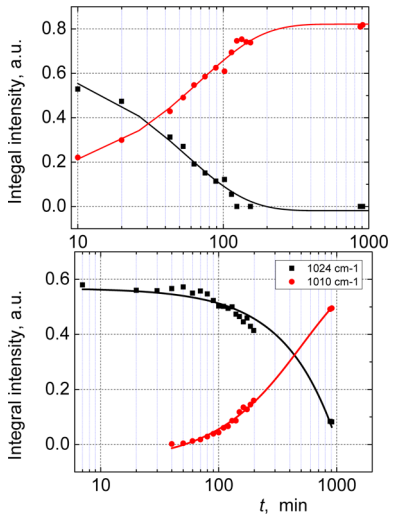

Figure 7. Kinetics of the H/D exchange reaction in $[C_{10}mim][X]$, X = Br (top) and Cl (bottom) in D_2O solution monitored using the integral intensities of Raman bands at 1010 and 1024 cm^{-1} (see Figure 6).

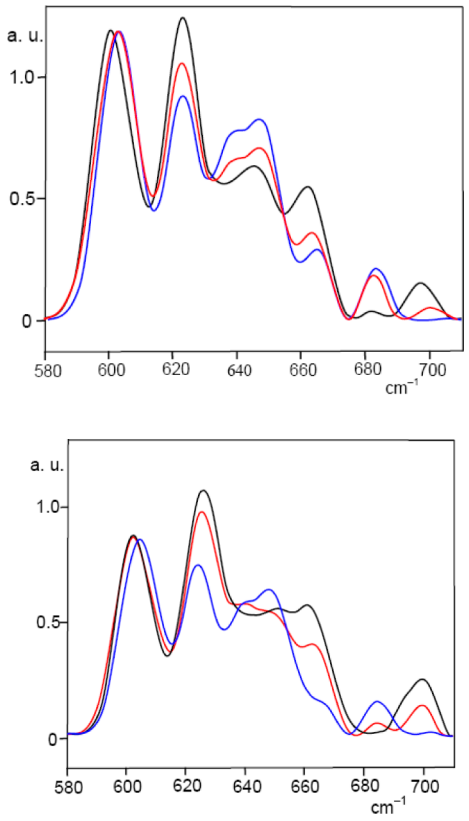

Figure 8. Time dependencies of Raman spectra in the range 600−700 cm^{-1} of $[C_{10}mim][X]$, X = Br (top; at 10 (black), 60 (red), and 150 (blue) min after the sample prepared) and Cl (bottom; at 20 (black), 220 (red), and 900 (blue) min) in D_2O solution (0.01 mole fraction of RTIL) at T = 296 K.

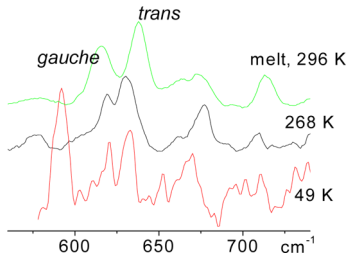

Figure 9. Raman spectra of $[C_{10}mim][Br]$ in the range 600−800 cm^{-1} in the liquid (296 K) and crystalline (268 and 49 K) phases.

systems (Figure 8). However, in the present case of $[C_{10}mim]^+$ (i.e. the cation with 10 carbons in the chain), it is somehow hardly credible to attribute this evolution being a completely conformational effect. Indeed, the Raman experiments carried out varying the temperature in the wide range on the neat $[C_{10}mim][Br]$ have revealed that the conformational composition was hardly changeable even passing through the melting and at further cooling up to 49 K (Figure 9). This behavior completely differs from the case of $[C_4mim][Cl]$ observed at the melting point and thermal equilibration at 72 °C.[40]

We are inclined to think that the complex redistribution of several Raman intensities (Figure 8) is due to the changes in positions of some strongly overlapping bands in this spectral range upon deuteration at C(2) site. To check this idea, vibrational modes in the range 500−700 cm^{-1} have been analyzed using DFT calculations on the *trans* and *gauche* conformers of the $[C_4mim]^+$ cation as a model system. Three different modeling schemes have been adopted. First, harmonic vibrational analysis was performed *in vacuo*. To account for the effects of aqueous environment, we have relied on the PCM as well as supermolecular approach,[43,44] where a hydrogen bonded complex of $[C_4mim]^+$ cation and a water molecule is placed into PCM void. The latter approach is believed to be particularly effective, since it accounts for both short- and long-range interactions simultaneously.[45] The calculated Raman spectra are shown in Figure 10. It is seen that for the *trans*-conformer the one of three bands (labeled as B in Figure 10), contributes the intensity of the neighboring band A. However, the band B shifts upon deuteration of C(2)−H to the lower wavenumbers (dashed arrows, Figure 10). Thus, the observed decrease of Raman intensity in the experimental spectra at 625 cm^{-1} (i.e. the band attributed to *trans*- conformer), (Figure 8) indeed can be explained by the shift of one of the overlapping

dx.doi.org/10.1021/jp4021245 | J. Phys. Chem. B 2013, 117, 10211−10220

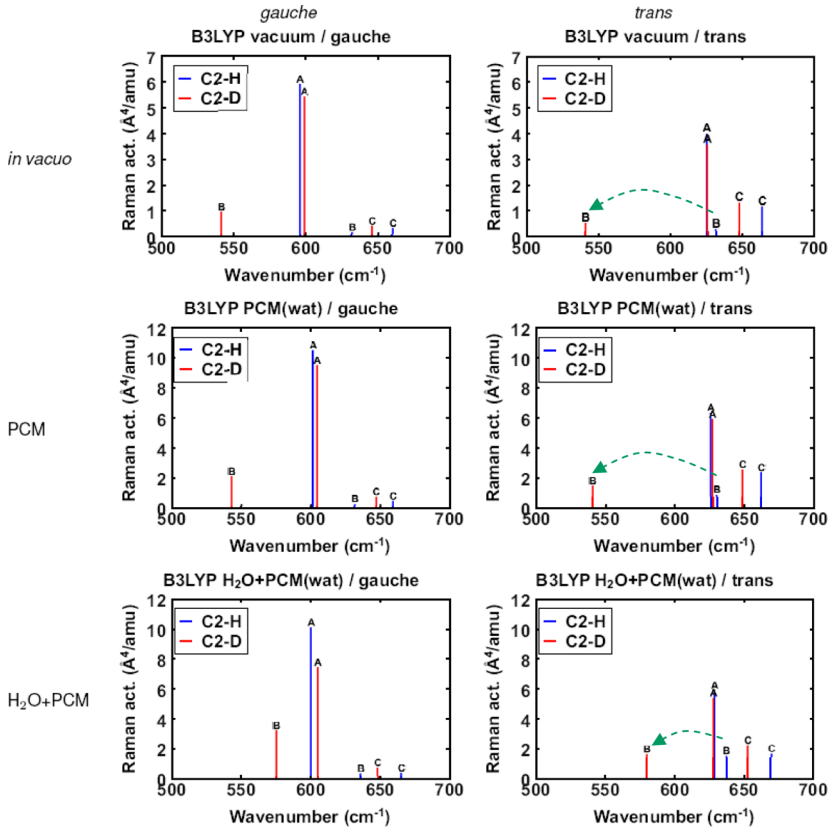

Figure 10. Raman modes of *gauche* and *trans* forms of $[C_4mim]^+$ calculated at the level B3LYP/6-311++G** *in vacuo*, in water as solvent using PCM, as well as for 'supermolecule' $[C_4mim]^+ \cdot H_2O$ in H_2O. More comments in text.

bands. This finding is qualitatively supported by all three modeling schemes used. The performed anharmonic analysis did not lead to the changes in the qualitative picture as well.

Discussion. The obtained results on the H/D exchange reaction rates should be discussed in more details. As it has been noted in ref 11, the interaction between the imidazolium cation and anion is strongly altered by the nature of the anions. On the one hand the smaller and more basic anions (i.e., Cl^- in the studied systems; ionic radii 1.81 Å) strengthen the H-bond as compared to the larger anions (Br^-, ionic radii 1.96 Å). The strengthening of H-bond should stimulate the larger amplitude motion of the proton. In the case of imidazolium-based RTILs, this motion could culminate producing carbene-like motif with a complete proton abstraction.[11,46] Hence, the exchange of proton by deuteron should go easier in the case of Cl^- anions. However, there are some other remarkable features that elucidate to behave the H-bond in the studied systems quite differently from the 'traditional' H-bonds. Such features are, for example, very weak and positive sloped dependence of the chemical shift of the C(2)−H proton on temperature $\Delta\delta/\Delta T \sim +10^{-3}$ ppm/deg, in comparison with $\Delta\delta/\Delta T \sim -10^{-2}$ ppm/deg for water and HDO,[35] the C(2)−H and C(4,5)−H stretching bands in FTIR spectra yielding a blue-shift with increasing dilution in water,[47] *etc.* It means that in this class of ionic liquids we deal with the H-bond systems that are 'inverted' respect to the traditional ones in the sense discussed in the Introduction. On the other hand, the anions in highly diluted aqueous solutions are solvated, and therefore, their role in H-bonding is significantly reduced. Moreover, the H/D exchange is coupled with the rotational dynamics of water molecules.[12] The interaction with anions hinders the rotational motion of D_2O molecules in the solvation shell and is the stronger the smaller the size of the anion. The activation energies for the rotational motion of water molecules in the hydration spheres of Cl^- and Br^- are 3.3 and 2.9 kcal/mol, respectively.[48] The rotational 'freezing' of D_2O molecules can hinder the supply of deuterons to the site of exchange. We assume that these are the main factors that cause only a small difference in the H/D exchange kinetics for both RTILs at high dilution (Figure 5, top graph), where the exchange is taking place between D_2O and the C(2)−H hydrogen of the cation and this process is mediated by the presence of the anion (i.e. Cl^- or Br^-).

The rotational motion of molecules and the diffusion are highly restricted in the liquid crystalline mesophases. Indeed, the H/D exchange was not observed in the gel mesophase, which was identified as liquid crystalline ionogel.[23,24,26] No changes in the spectra have been observed even after 48 days from the sample preparation.

The H/D exchange can be discussed in the terms of the ion pairing.[49,50] The importance of this process for ionic liquids was studied very recently.[50] It was shown that there exists a certain "magic number" of water molecules that is necessary to disrupt the strongly bound ion pairs (contact ion pairs, CIP) initiating their transition to the solvent-separated state (solvent-separated ion pairs, SIPs). For instance, for some protic ionic liquids, it was determined that a minimum of four water molecules were needed to initiate the transition from CIPs to SIPS.[50] It was also noted that this process strongly depends on the anions, and it is expected that for other RTILs such transition may begin at lower water content. Unfortunately, the "magic number" of water molecules is not known for $[C_{10}mim][X]$,

dx.doi.org/10.1021/jp4021245 | J. Phys. Chem. B 2013, 117, 10211−10220

X = Br, Cl solutions in D_2O. Intuitively, it could be supposed that it should be slightly below CAC. Hence, two extreme cases of the present studies, that is, the mixtures at high dilution (10^{-4} mole fraction of RTIL) and in the gel phase (0.4 mole fraction of RTIL), can be considered as the ionic systems being in SIP and CIP states, respectively. The strong anion−cation interaction impedes the H/D exchange process in the gel phase. This factor can be considered as additional contribution to the slowdown of rotational dynamics discussed just above.

The most complex situation appears between these two extreme cases, that is, at the compositions slightly above CAC. The kinetics of H/D exchange drastically changes in the samples of ∼0.01 mole fraction of RTIL (Figure 5). This process, depending on the anions, can be very significantly damped ([C_{10}mim][Cl]) or stimulated ([C_{10}mim][Br]). Unfortunately, it is virtually unknown how certain inherent properties of RTIL influence the self-aggregation and phase behavior of RTIL/water solutions. Theoretical modeling presented in ref 28 has revealed that the micelle sizes and shapes depend on the counterion type and alkyl chain length but also on the number molecules that are involved in the modeling. Water molecules can be trapped in different environments and dictate the shape and size of the aggregates.[28] Various aspects of micelle formation and structure have been explored experimentally by SANS, NMR, fluorescence, surface tension, and conductivity measurements and other techniques.[28,31,32,51−54] It was demonstrated that general features of micellar aggregation of long-chain imidazolium-based RTILs in aqueous solutions are rather similar to those of conventional ionic surfactants having the same hydrocarbon chains.[31,51] Higher inclination for aggregation and thus the lower values of CAC of RTILs can be attributed to the capability of imidazolium groups to form H-bonds with anions.[51] Beside CAC, micelle formation can be characterized by other important parameters such as shape and size, aggregation number, degree of counterion binding, *etc.* Regrettably, not all of these parameters can be collected from the literature for [$C_n$mim][X] with n = 10, X = Br and Cl in aqueous solution which were studied in the present work. Therefore, data for closely related RTILs (e.g. for those with n = 8 − 12 or $X = I^-$, BF_4^-) have to be taken and used for discussion.

Namely, it was deduced that the effect of anions X = Br^- and BF_4^- on the degrees of counterion binding of [$C_n$mim][X] with n = 10 and 12 in water was minor,[32] even though these anions differ in their size and hydrophobicity very significantly. The effect of anions is, however, significant for the size, aggregation number (N_{agg}), and shape of micelles.[52−54] For example, micelles formed in [C_8mim][I] solutions possess over the concentration range for which the structure of aggregates is more or less stable the core radii of 13.2 ± 0.5 Å and $N_{agg} \approx 40$, to be compared to 10.5 ± 0.5 Å and $N_{agg} \approx 20$ for [C_8mim][Br] or 13.4 ± 0.4 Å and $N_{agg} \sim 33 - 45$ for [C_{10}mim][Br] solutions, respectively.[52−54] Also, aggregates in [$C_n$mim][X] systems containing $X = Br^-$ and I^- were found to be nearly spherically shaped. The micelles in [C_{10}mim][Br] solutions become increasingly elongated with increasing RTIL concentration.[54] In contrast to bromine and iodide systems, the [C_8mim][Cl] in aqueous solution appears to form disk-like rather than spherical aggregates.[53,54]

Nevertheless, this data does not provide an answer to the question of why Br^- and Cl^- anions could so crucially influence the H/D exchange reaction rates above CAC. It is likely possible that this is indeed a much finer phenomenon related to the microscopic (short-range) ordering and molecular microdynamics, in particular, that of water molecules. SANS experiments on aqueous solutions of [C_8mim][Cl] suggest the presence of some structures with interdigitated alkyl chains, the ordering of micellar rods, or the formation of sheets of bilayers.[53] Moreover, at moderate concentrations, the long-range order between [C_8mim][Cl] aggregates is more pronounced than in the [C_8mim][I] solutions.[53] The patterns of deuteron quadrupolar splitting in ^{2}H NMR spectra provide extremely valuable information on this. The ^{2}H NMR experiments carried out using deuterated species of [$C_n$mim]-[X], n = 8 and 10, X = Br^- and Cl^- in aqueous solutions have revealed that (i) Cl^- is more strongly solvated than Br^- and thus the D_2O molecules are residing in a more ordered environment in the case of [$C_n$mim][Cl]; (ii) larger anions, viz. Br^-, are less tightly bound to the micelle surface and thus enhanced repulsive interactions can destabilize the mesophase.[54] This conclusion is in fact entirely consistent with our observations, namely greater ordering and much slower dynamics in the gel phase is more clearly pronounced on the ^{1}H NMR signal shapes of [C_{10}mim][Cl] than in the case of [C_{10}mim][Br] gel, as illustrated in Figure 3. It is obvious that these observations first of all highlight the effect of the anions on the differential mesophase properties of studied RTIL/water solutions. However, it is reasonable to expect a certain phase memory, namely, more ordered mesophase can grow from more ordered building units (i.e., micelles).

We would like to conclude that a higher degree of molecular freedom due to the order−disorder effects plays the crucial role in the H/D exchange reaction in the studied systems. The presented experimental results are expected to be useful for the molecular design of ionic liquids and the modeling of micellar structures in aqueous solutions.

The conformational changes that can be coupled with the H/D exchange, as it was observed in ref 15, do not occur in the studied systems. The complex redistribution of several Raman intensities (Figure 8) can be due to the frequency shifts of some strongly overlapped bands upon the H/D exchange. More rigorously, this idea can be rejected in the light of ^{13}C NMR results. For this purpose, the ^{13}C NMR shielding tensors of *trans* and *gauche* forms of $[C_4mim]^+ \cdot H_2O$ 'supermolecule' in H_2O, again as a model system, have been calculated at the level of PBE0/6-311++G(2d,2p)/PCM. We have utilized and checked this theoretical approach in our previous studies, where it was found that the PBE0 functional applied together with the polarizable continuum model (PCM) gives very good agreement between calculated and experimental ^{1}H and ^{13}C chemical shifts and perfectly reproduces many observed tendencies, for H-bonded systems in particular.[6,55,56] The calculated isotropic parts of ^{13}C NMR shielding tensors are given in Table 3. It follows that if *trans*−*gauche* conformational transition really runs in the studied RTILs it would be easily noticeable in ^{13}C NMR spectra: the spectral distancing between C(4) and C(5) signals should increase ∼1.5 ppm, even more significant shifts should be observed for the carbons in the hydrocarbon chain, for example, − 3.4 ppm for C(8), (Table 3). Nothing like this has been observed in spectra. Thus, the observed changes (Table 2) indeed can be attributed to the secondary (^{13}C) isotope effects, the values of which are comparable with those determined for many other H-bond systems,[37,38] than to suppose that the signal shifts are due to the conformational *trans*−*gauche* transition.

Table 3. Isotropic Parts of ^{13}C NMR Shielding Tensors (σ) of *trans* and *gauche* Forms of $[C_4mim]^+$ Calculated at the Level of PBE0/6-311++G(2d,2p)/PCM using $[C_4mim]^+ \cdot H_2O$ 'Supermolecule' in H_2O as Solvent and the Predictable Shifts of Corresponding Carbon Signals in NMR Spectra ($\Delta\sigma$) Due to the Conformational Changes (all in ppm)

carbon no.	σ_{trans}	σ_{gauche}	$\Delta\sigma = \sigma_{trans} - \sigma_{gauche}$
C(2)	45.12	44.43	+ 0.69
C(4)	59.07	60.25	− 1.18
C(5)	58.78	58.37	+ 0.41
C(6)	150.52	150.53	− 0.01
C(7)	133.38	133.34	+ 0.04
C(8)	149.44	152.81	− 3.37

CONCLUSIONS

The anions and aggregation effects play crucial role in RTIL aqueous solutions. The anions interact with cations via H-bonds and bind the water molecules in their solvation shells. The overlap and the competition of these processes may cause rather complex dependency of the H/D exchange reaction rate on the sample composition and on other experimental conditions (temperature, degree of purification, *etc.*). The H/D exchange process, depending on the anions, can be very significantly damped or stimulated above critical aggregation (micellization) concentration. This reaction does not run in the liquid crystalline gel phase.

The concept of the conformational changes coupled with the H/D exchange in $[C_{10}mim][X]$, X = Br and Cl, maybe also in others imidazolium-based RTILs with longer hydrocarbon chains, can be rejected by ^{13}C NMR data. The revealed changes in ^{13}C NMR spectra are caused by the secondary isotope effects on chemical shifts not being the signal shifts due to the conformational *trans*−*gauche* transition.

AUTHOR INFORMATION

Corresponding Author

*E-mail: vytautas.balevicius@ff.vu.lt.

Notes

The authors declare no competing financial interest.

ACKNOWLEDGMENTS

The study was funded from the European Community's social foundation under Grant Agreement No. VP1-3.1-ŠMM-08-K-01-004/KS-120000-1756.

REFERENCES

(1) *Ionic Liquids in Synthesis*, 2nd ed.; Wasserscheid, P., Welton, T., Eds.; Wiley-VCH: Weinheim, 2008.
(2) Wishart, J. F.; Castner, E. W. The Physical Chemistry of Ionic Liquids. *J. Phys. Chem. B* **2007**, *111* (18), 4639−4640.
(3) Fukushima, T.; Aida, T. *Chem.—Eur. J.* **2007**, *13*, 5048−5058.
(4) *Electrochemical Aspects of Ionic Liquids*; Ohno, H., Ed.; John Wiley: Hoboken, NJ, 2005.
(5) Fumino, K.; Wulf, A.; Ludwig, R. *Angew. Chem., Int. Ed.* **2008**, *47*, 8731−8734.
(6) Balevicius, V.; Gdaniec, Z.; Aidas, K. *Phys. Chem. Chem. Phys.* **2009**, *11*, 8592−8600.
(7) Balevicius, V.; Bariseviciute, R.; Aidas, K.; Svoboda, I.; Ehrenberg, H.; Fuess, H. *Phys. Chem. Chem. Phys.* **2007**, *9*, 3181−3189.
(8) Szafran, M. *J. Mol. Struct.* **1996**, *381*, 39−64.
(9) Koeppe, B.; Tolstoy, P. M.; Limbach, H. H. *J. Am. Chem. Soc.* **2011**, *133*, 7897−7908.
(10) Balevicius, V.; Aidas, K.; Svoboda, I.; Fuess, H. *J. Phys. Chem. A* **2012**, *116*, 8753−8761.
(11) Cremer, T.; Kolbeck, C.; Lovelock, K. R. J.; Paape, N.; Woelfel, R.; Schulz, P. S.; Wasserscheid, P.; Weber, H.; Thar, J.; Kirchner, B.; Maier, F.; Steinrueck, H. P. *Chem.—Eur. J.* **2010**, *16*, 9018−9033.
(12) Yasaka, Y.; Wakai, C.; Matubayasi, N.; Nakahara, M. *J. Phys. Chem. A* **2007**, *111*, 541−543.
(13) Ohta, S.; Shimizu, A.; Imai, Y.; Abe, H.; Hatano, N.; Yoshimura, Y. *Open J. Phys. Chem.* **2011**, *1*, 70−76.
(14) Nakakoshi, M.; Ishihara, S.; Utsumi, H.; Seki, H.; Koga, Y.; Nishikawa, K. *Chem. Phys. Lett.* **2006**, *427*, 87−90.
(15) Hatano, N.; Watanabe, M.; Takekiyo, T.; Abe, H.; Yoshimura, Y. *J. Phys. Chem. A* **2012**, *116*, 1208−1212.
(16) Dontsov, S.; Shemetova, E. S.; Chernyshev, Y. S. *Abstracts of NMRCM-2012*, 9−13 July, Saint Petersburg, Russia, p 75.
(17) *Almanac*; Bruker-Biospin: Billerica, MA, 2011; p. 22.
(18) Frisch, M. J.; Trucks, G. W.; Schlegel, H. B.; Scuseria, G. E.; Robb, M. A.; Cheeseman, J. R.; Scalmani, G.; Barone, V.; Mennucci, B.; Petersson, G. A. et al. *Gaussian* 09, revision C.01; Gaussian, Inc., Wallingford, CT, 2010.
(19) Becke, A. D. *J. Chem. Phys.* **1993**, *98*, 5648−5652.
(20) Krishnan, R.; Binkley, J. S.; Seeger, R.; Pople, J. A. *J. Chem. Phys.* **1980**, *72*, 650−654.
(21) Tomasi, J.; Mennucci, B.; Cammi, R. *Chem. Rev.* **2005**, *105*, 2999−3093.
(22) Barone, V. *J. Chem. Phys.* **2005**, *122*, 014108(10).
(23) Firestone, M. A.; Dzelawa, J. A.; Zapol, P.; Curtiss, L. A.; Seifert, S.; Dietz, M. L. *Langmuir* **2002**, *18*, 7258−7260.
(24) Inoue, T.; Dong, B.; Zheng, L. Q. *J. Colloid Interface Sci.* **2007**, *307*, 578−581.
(25) Balevicius, V.; Gdaniec, Z.; Aidas, K.; Tamuliene, J. *J. Phys. Chem. A* **2010**, *114*, 5365−5371.
(26) Balevicius, V.; Dziaugys, L.; Kuliesius, F.; Marsalka, A. *Lith. J. Phys.* **2011**, *51*, 212−220.
(27) Blesic, M.; Marques, M. H.; Plechkova, N. V.; Seddon, K. R.; Rebelo, L. P. N.; Lopes, A. *Green Chem.* **2007**, *9*, 481−490.
(28) Singh, T.; Kumar, A. *J. Phys. Chem. B* **2007**, *111*, 7843−7851.
(29) Zhao, Y.; Gao, S.; Wang, J.; Tang, J. *J. Phys. Chem. B* **2008**, *112*, 2031−2039.
(30) Jungnickel, C.; Luczak, J.; Ranke, J.; Fernandez, J. F.; Mueller, A.; Thoeming, J. *Colloids Surf., A* **2008**, *316*, 278−284.
(31) Dong, B.; Zhao, X.; Zheng, L.; Zhang, J.; Li, N.; Inoue, T. *Colloids Surf., A* **2008**, *317*, 666−672.
(32) Dong, B.; Li, N.; Zheng, L.; Inoue, T. *Langmuir* **2007**, *23*, 4178−4182.
(33) Sirieix-Plenet, J.; Gaillon, L.; Letellier, P. *Talanta* **2004**, *63*, 979−986.
(34) Jeon, Y.; Sung, J.; Seo, C.; Lim, H.; Cheong, H.; Kang, M.; Moon, B.; Ouchi, Y.; Kim, D. *J. Phys. Chem. B* **2008**, *112*, 4735−4740.
(35) Balevicius, V.; Gdaniec, Z.; Dziaugys, L.; Kuliesius, F.; Marsalka, A. *Acta Chim. Slov.* **2011**, *58*, 458−464.
(36) Remsing, R. C.; Wildin, J. L.; Rapp, A. L.; Moyna, G. *J. Phys. Chem. B* **2007**, *111*, 11619−11621.
(37) Stare, J.; Jezerska, A.; Ambrozic, G.; Kosir, I.; Kidric, J.; Koll, A.; Mavri, J.; Hadzi, D. *J. Am. Chem. Soc.* **2004**, *126*, 4437−4443.
(38) Dziembowska, T.; Hansen, P. E.; Rozwadowski, Z. *Progr. Magn. Res. Spectrosc.* **2004**, *45*, 1−29.
(39) Berg, R. W.; Deetlefs, M.; Seddon, K. R.; Shim, I.; Thompson, J. M. *J. Phys. Chem. B* **2005**, *109*, 19018−19025.
(40) Berg, W. R. *Monatsh. Chem.* **2007**, *138*, 1045−1075.
(41) Wulf, A.; Fumino, K.; Ludwig, R. *J. Phys. Chem. A* **2010**, *114*, 685−686.
(42) Lassegues, J. C.; Grondin, J.; Cavagnat, D.; Johansson, P. *J. Phys. Chem. A* **2010**, *114*, 687−688.
(43) Noell, J. O.; Morokuma, K. *Chem. Phys. Lett.* **1975**, *36*, 465−469.
(44) Mikkelsen, K. V.; Luo, Y.; Ågren, H.; Jørgensen, P. *J. Chem. Phys.* **1995**, *102*, 9362(7).

(45) Mennucci, B.; Martinez, J. M.; Tomasi, J. *J. Phys. Chem. A* **2001**, *105*, 7287−7296.
(46) Arduengo, A. J., III; Dixon, D. A.; Kumashiro, K. K.; Lee, C.; Power, W. P.; Zilm, K. W. *J. Am. Chem. Soc.* **1994**, *116*, 6361−6367.
(47) Gao, Y.; Zhang, L.; Wang, Y.; Li, H. *J. Phys. Chem. B* **2010**, *114*, 2828−2833.
(48) Endom, L.; Hertz, H. G.; Tuehl, B.; Zeidler, M. D. *Ber. Bunsen-Ges. Phys. Chem.* **1967**, *71*, 1008−1031.
(49) Marcus, Y.; Hefter, G. *Chem. Rev.* **2006**, *106*, 4585−4621.
(50) Stange, P.; Fumino, K.; Ludwig, R. *Angew. Chem., Int. Ed.* **2013**, *52*, 2990−2994.
(51) Inoue, T.; Ebina, H.; Dong, B.; Zheng, L. Q. *J. Colloid Interface Sci.* **2007**, *314*, 236−241.
(52) Wang, J.; Wang, H.; Zhang, S.; Zhang, H.; Zhao, Y. *J. Phys. Chem. B* **2007**, *111*, 6181−6188.
(53) Bowers, J.; Butts, C. P.; Martin, P. J.; Vergara-Gutierrez, M. C.; Heenan, R. K. *Langmuir* **2004**, *20*, 2191−2198.
(54) Goodchild, I.; Collier, L.; Millar, S.; Prokes, I.; Lord, J. C. D.; Butts, C. P.; Bowers, J.; Webster, J. R. P.; Heenan, R. K. *J. Colloid Interface Sci.* **2007**, *307*, 455−468.
(55) Aidas, K.; Marsalka, A.; Gdaniec, Z.; Balevicius, V. *Lith. J. Phys.* **2007**, *47*, 443−449.
(56) Balevicius, V.; Balevicius, V. J.; Aidas, K.; Fuess, H. *J. Phys. Chem. B* **2007**, *111*, 2523−2532.